HHS Public Access

Author manuscript

Free Radic Biol Med. Author manuscript; available in PMC 2024 July 01.

Published in final edited form as:

Free Radic Biol Med. 2023 July ; 203: 34–44. doi:10.1016/j.freeradbiomed.2023.03.262.

Mitochondrial OGG1 expression reduces age-associated neuroinflammation by regulating cytosolic mitochondrial DNA

Mansoor Hussain[1], **Xixia Chu**[1], **Burcin Duan Sahbaz**[1], **Samuel Gray**[1], **Komal Pekhale**[1], **Jae-Hyeon Park**[1], **Deborah L. Croteau**[1,2], **Vilhelm A. Bohr**[1,3]

[1]DNA repair section, National Institute on Aging, Baltimore, Maryland, USA 21224

[2]Computational Biology & Genomics Core, National Institute on Aging, Baltimore, Maryland, USA 21224

[3]Danish Center for Healthy Aging, University of Copenhagen, Copenhagen 2200, Denmark

Abstract

Aging is accompanied by a decline in DNA repair efficiency, which leads to the accumulation of different types of DNA damage. Age-associated chronic inflammation and generation of reactive oxygen species exacerbate the aging process and age-related chronic disorders. These inflammatory processes establish conditions that favor accumulation of DNA base damage, especially 8-oxo-7,8 di-hydroguanine (8-oxoG), which in turn contributes to various age associated diseases. 8-oxoG is repaired by 8-oxoG glycosylase1 (OGG1) through the base excision repair (BER) pathway. OGG1 is present in both the cell nucleus and in mitochondria. Mitochondrial OGG1 has been implicated in mitochondrial DNA repair and increased mitochondrial function. Using transgenic mouse models and cell lines that have been engineered to have enhanced expression of mitochondria-targeted OGG1 (mtOGG1), we show that elevated levels of mtOGG1 in mitochondria can reverse aging-associated inflammation and improve functions. Old male mtOGG1^{Tg} mice show decreased inflammation response, decreased TNFx levels and multiple pro-inflammatory cytokines. Moreover, we observe that male mtOGG1^{Tg} mice show resistance to STING activation. Interestingly, female mtOGG1^{Tg} mice did not respond to mtOGG1 overexpression. Further, HMC3 cells expressing mtOGG1 display decreased release of mtDNA into the cytoplasm after lipopolysacchride induction and regulate inflammation through the pSTING pathway. Also, increased mtOGG1 expression reduced LPS-induced loss of mitochondrial functions. These results suggest that mtOGG1 regulates age-associated inflammation by controlling release of mtDNA into the cytoplasm.

Correspondence: Vilhelm Bohr (vbohr@sund.ku.dk).

AUTHOR CONTRIBUTIONS

M.H. performed most of the experiments, data analysis and wrote manuscript. MH, XC, SG, KP and JHP performed experiments. BD performed western blots. M.H, D.L.C., and V.A.B conceived and designed the research. M.H., D.L.C. and V.A.B. wrote the manuscript.

INTRODUCTION

Aging is a universal complex phenomenon affecting stochastic, genetic, and cellular functions in multiple cell types and tissues, with the immune system undergoing multiple profound changes. This age-associated dysregulation of the immune system results in increased circulating pro-inflammatory cytokines including Interleukin 6 (IL-6) and tumor necrosis factor alpha (TNFα) and acute phase protein in older people even without infection[1]. The low level of chronic inflammation in aging is called “inflammaging”[2–4]. The persistent inflammaging causes tissue damage and results in more inflammation leading to a vicious cycle of inflammaging and age-related diseases including cardiovascular diseases, atherosclerosis, dementia, and Alzheimer’s disease[5]. The brain has a highly regulated adaptive immune system to clear pathogens. However, in the context of inflammaging, the brain becomes more vulnerable leading to a dysregulated neuro-immune axis. Triggered inflammation in the brain is observed in many age-related neurological disorders[6]. However, the precise mechanism of age-related chronic inflammation and tissue dysfunction in the brain is not understood.

DNA is continuously damaged during the aging process in which numerous exogenous and endogenous genotoxins increase. Genomic instability due to DNA damage accumulation is a hallmark of aging and has been linked to DNA mutations and cognitive impairment[7, 8]. Interestingly, mutations in DNA repair genes and impaired DNA repair pathways are linked to premature aging in both humans and rodents[9, 10]. Aged cells also show an increase in reactive oxygen species (ROS) leading to oxidative damage in the nuclear and mitochondrial genomes[11, 12]. ROS induces high levels of 8-oxoG in the mitochondrial genome[13, 14] and 8-oxoguanine DNA glycosylase-1 (OGG1) removes 8-oxoG lesions from DNA. It localizes to both the nucleus and mitochondria[15]. Mutational studies on *OGG1*$^{-/-}$ mice showed accumulation of 8-oxoG levels in both nuclear and mitochondrial DNA[16]. Previous studies have shown that mRNA and protein levels of OGG1 decrease with age in mouse brain[17] and the import of OGG1 into mitochondria decrease with age[18]. Interestingly, it has been shown that the mitochondrial OGG1 increase is protective against Alzheimer disease-like pathologies[19]. In addition, according to the studies conducted in recent years, release of damaged mitochondrial DNA into the cytoplasm is one of the known events that trigger inflammation in neurological diseases through the cGAS-STING signaling cascades [20–22]. Given the age dependent decline of mitochondrial OGG1, we were interested in understanding the role of mitochondrial OGG1 relative to the age-associated chronic inflammation in aging brain. To this end, we used microglial cells in culture and naturally aged transgenic mice constitutively expressing elevated levels of human mitochondria-targeted OGG1 (mtOGG1)[23]. Mice with this genotype are hereafter referred to as mtOGG1^{Tg}. Here we show that mtOGG1 expression alone confers a protective role in age-associated inflammation. Our results indicate that mtOGG1 plays a role in the inflammatory response, and in mitochondrial metabolism via regulating release of mitochondrial DNA (mtDNA) to the cytoplasm in vivo and in human microglial cell lines.

MATERIALS AND METHODS

Animals

The construction and characterization of mtOGG1^{Tg} mice were previously described [23–26] and were a gift from R. Stephen Lloyd, Oregon Health & Science University. These mice express the human OGG1-1a isoform, which has been previously modified for mitochondrial localization using sequences derived from the *MnSOD* gene which drives increased mitochondrial OGG1 activity without elevated levels detectable in nuclear OGG1. Mice were produced by mating between male and female transgenics, and all breeding and care of animals were in accordance with the protocols approved by the Animal Care and Use Committee of Oregon Health & Science University, Portland, Oregon. Following transfer of mice from OHSU to NIA, all breeding and care of animals were in accordance with the protocols approved by the Animal Care and Use Committee of the National Institute on Aging. Mice were fed ad libitum and were on a 12h light dark cycle.

Cell lines and transfection

Human microglial cells (HMC3) were grown in EMEM media (Gibco) containing 10% FBS and Pen-Strep 50 I.U./mL penicillin and 50 (μg/mL) streptomycin at 37°C in a 5% CO_2 humidified incubator. Cells were purchased from ATCC and tested for mycoplasma. For the generation of mtOGG1 stable cell lines, HMC3 cells were transfected with the pCMV/myc/mito-hOGG1 or vector plasmids using Lipofectamine plus (Invitrogen, Life Technologies) per manufacturer's directions. Post 48 hours transfection, cells were screened using G418 (400ug/mL). The presence of exogenous OGG1 was confirmed using anti-Myc tag antibody in mitochondrial fraction.

RNA isolation and Nanostring ncounter

NanoString analysis was performed on the hippocampus of mtOGG1^{Tg} and WT mice. Total RNA was purified with a PureLink™ RNA Mini Kit (Thermo Fisher Scientific, #12183018A) as per the manufacturer's protocol. Purified RNA was quantified on a NanoDrop ND-1000 spectrophotometer and diluted in nuclease-free water to 20 ng/uL. The Nanostring neuroinflammation panel v1 was employed to study the changes in gene expression related to neuroinflammation. The panel contains 757 genes covering the core pathways and processes that define neuroimmune interactions, and 13 internal reference genes for data normalization. It was hybridized in CodeSet Master mix carrying hybridization buffer, Reporter Code Set, and Capture Probe Set for 16 to 24 hours at 65°C (NanoString Technologies, MAN-10056-05) and thenapplied to the nCounter Prep Station. The hybridized RNA was loaded onto the nCounter Prep Station for immobilization in the sample cartridge according to the manufacturer's high sensitivity protocol (MAN-C0035). The sample cartridge was subsequently processed for 2.5 hours in the nCounter Analysis System. Next, the nCounter Digital Analyzer which was a multichannel epifluorescence scanner collected data by taking images of the immobilized fluorescent reporters in the sample cartridge with a CCD camera through a microscope objective lens. The results were directly downloaded from the digital analyzer in RCC files format. NanoString Advanced analysis (nSolver 4.0) was used for data analysis. Genes with a fold-change cut-off of ≥|0.5| and p-value less than 0.05 were considered statistically significant. No genes were

significant after multiple testing. Pairwise T-test was used to determine which pathways were significant with p-values of less than 0.05 considered significant.

Immunoblotting

Cell extracts were prepared with RIPA lysis buffer (Thermo scientific pierce) containing protease inhibitor cocktail (Thermo Scientific Pierce) and nuclease (0.1U/uL). Lysates were clarified by centrifugation at 14000 xg at 4°C and 50–100 ug of the cell extracts were boiled in 4X LDS dye (Invitrogen). Samples were loaded on SDS-PAGE gels (Invitrogen) and then transferred to PVDF membranes. Membranes were blocked with 5% nonfat milk in TBST for 45 min at RT followed by incubation with indicated a primary antibody overnight at 4°C. The HRP-conjugated secondary antibodies (Cell Signaling Technologies) were added to the membranes. Blots were developed using the ECL western blotting substrate (Perkin Elmer) and images were obtained via the Bio-Rad ChemiDoc. The antibodies used in the study are STING (13647, CST), Phospho-STING (Ser366) (E9A9K) (50907, CST), cGAS (D1D3G) (15102, CST), IL-6 (D3K2N) (12153, CST), IL-8 (E5F5Q) (94407, CST), TNF-α Antibody (3707, CST), IBA1 (019-19741, WAKO chemicals), IL1B (12242, CST), P62 (5114S, CST), ACTIN (SC-47778, Santa cruz), pSTING (72971S, CST) and STING (13647S, CST).

Immunofluorescence staining

Mice were deeply anesthetized by isoflurane and then perfused with 1× phosphate buffered saline (PBS) through the heart. Brains were removed from the skull, fixed in 4% paraformaldehyde (PFA) for 24 h at 4 °C, and dehydrated in 30% sucrose in PBS solution for 24–48 h until sunk to the bottom. Coronal brain sections were obtained by a cryostat (Tissue-Tek cryo, Flex) at 20 μm and every eight sections were collected in one well. The sections were placed on the slide and treated with RNAse A (5mg/mL) for 60mins at 37°C. slides were then washed gently three times with 1X PBS and blocking was performed in 5% donkey serum and 0.3% Triton X-100 in PBS solution for 1 h at room temperature. Slides were gently washed three times with 1xPBS for 10 min each, followed by overnight incubation with the primary antibody at 4 °C. After three 10 min washes in PBS, slides were incubated with the appropriate fluorescent probe-conjugated secondary antibodies for 1 h at room temperature while protected from light. mtOGG1 stable and mock cells were either treated with lipopolysaccharide (LPS) or vehicle. 4 Hr after the treatment, immunostaining was performed for the presence of cytosolic dsDNA. Nuclei were stained with 4,6-diamidino-2-phenylindole (DAPI) with mounting medium (Fisher Scientific, #P36962). Pictures were taken using an Axiovert 200M microscope (ZEISS) or a Leica confocal microscope scanner (Aperio versa 200). The specific primary antibodies used include AIF-1/Iba1 (1:500, WAKO, #019-19741), NeuN (1:250, Millipore Sigma, # MAB377), Doublecortin (1:250, Cell Signaling Technology, #4604), dsDNA (1:250, Sigma, #MAB1293) and 8-oxoG antibody (1:500, Millipore, #MAB3560). Image analysis and quantification were performed using ImageJ.

Subcellular fractionation

Subcellular fractionation and mitochondrial DNA quantification were adapted and modified from previous studies [27, 28]. HMC3 cells expressing mtOGG1 or vector were lysed in MS buffer (225 mM Mannitol, 75 mM Sucrose, 5 mM Hepes, 1 mM EGTA, 0.1% Fatty acid free

BSA, with the pH adjusted to 7.4 with KOH) and incubated on a rotator at 4°C. Samples were centrifuged at 2,200 g for 3 min at 4°C. The cytosolic fractions were generated by centrifugation of the supernatants at 22,000 g for 10 min at 4°C and transferring supernatants to fresh tubes. The pellet was resuspended in 1 ml mitochondrial suspension (MS) buffer and centrifuged at 22,000 g for 10 min at 4°C, with the pellet constituting the mitochondrial fraction. DNA was subsequently extracted from the appropriate cytosolic and mitochondrial fractions using the QIAmp DNA Mini Kit (QIAGEN Cat 51304). Cytosolic and mitochondrial DNA were used for qPCR analysis using gene-specific primers. The primers used to amplify each transcript are as follows: mt-ND1 (forward: 5'-CACCCAAGAACAGGGTTTGT-3' and reverse: 5'-TGG CCATGGGTATGTTGTTAA-3'), mt-DLOOP (5'-CTATCACCCTATTAACCACTCA-3' and reverse: 5'-TTCGCCTGTAATATTGAACGTA-3'), mt-CO2 (5'-AATCGAGTAGTACTCCCGATTG-3' and reverse: 5'-TTCTAGGACGATGGGCATGAAA-3'), mt-ATP6 (5'-AATCCAAGCCTACGTTTTCACA-3' and reverse: 5'-AGTATGAGGAGCGTTATGGAGT-3').

Mitochondrial respiration analysis

The oxygen consumption rate (OCR) was assessed using a Seahorse Bioscience XF96 analyzer (Seahorse Bioscience, Billerica, MA, USA). MtOGG1 stable and mock HMC3 cells were seeded in the XF96 cell culture microplate (Seahorse Bioscience, Cat# 102601-100) and grown to 80% confluency in 200 μL of growth medium prior to analysis. On the day of the assay, culture media were changed to assay medium with 175 μL (Dulbecco's Modified Eagle's Medium, Cat# 12800 – 017). Prior to assay, plates were incubated in a non-CO_2, 37 °C incubator for 30 min. Thereafter successive OCR measurements were aquired consisting of basal OCR, followed by OCR level after the automated injection of 25 μL oligomycin (10 μM), 25 μL carbonyl cyanide 4-(trifluoromethoxy) phenylhydrazone (FCCP) (1 μM), and a combination of 25 μL rotenone + antimycin A (1 μM), respectively. After plate reading, cells were carefully washed with PBS and lysed with 1X RIPA lysis buffer (50mM Tris–HCl, pH 7.4, 150mM NaCl, 1mM EDTA, 1mM EGTA, 1.2% Triton X-100, 0.5% sodium deoxycholate, and 0.1% SDS, Enzo Life Sciences, Cat# ADI-80-1496) containing protease inhibitors cocktail (Roche, Indianapolis, IN, USA). Then, proteins were quantified by the Bradford assay. OCR determination was normalized by the protein concentration of its respective well.

8-oxo-dG ELISA

HMC3 WT or mtOGG1 cells were grown and treated with or without LPS treatment for 6 hours. Mitochondrial DNA was isolated as described previously[28]. DNA was extracted using the DNA minikit (Qiagen) according to the manufacturer's instructions. 8-oxo-dG was quantified using the HT 8-oxo-dG enzyme-linked immunosorbent assay (ELISA) kit II (R&D systems Cat#4380-192-K). Samples were assayed in biological triplicate.

Data

GEO Accession GSE227426

RESULTS

Male mice expressing enhanced levels of mtOGG1 exhibit reduced inflammation in the hippocampus

Age-associated immune dysregulation leads to elevated levels of pro-inflammatory markers that can trigger frailty and premature death [1–3]. To assess the role of mitochondrial OGG1 in inflammation-related gene expression changes due to aging, we employed the NanoString's Neuroinflammation panel. This panel contains 757 genes associated with neuroinflammation and 23 neuroinflammatory pathways. NanoString analysis was carried out using total RNA isolated from the hippocampus of mice brains. We further analyzed the correlation of pathway scores that are altered between aged mtOGG1^{Tg} with regard to WT mice, and the matrix indicated that mtOGG1^{Tg} male mice conferred significant changes in gene expression compared to WT aged mice (Figure 1A). Interestingly, females did not show any differences across the genotypes (Figure 1B). Next, we investigated individual terms affected by mtOGG1 expression among male mice. As shown in Figure 1C, mtOGG1^{Tg} male mice showed significant changes in pathway scores including increases in growth factor signaling and astrocyte function, and decreases in inflammatory signaling, innate and adaptive immune responses, and cellular stress but female mtOGG1^{Tg} mice did not show significant differences (Figure 1D). Figure 1E heatmap shows differentially expressed genes in aged mtOGG1^{Tg} when compared to age-matched control mice. Together, these results suggest that enhanced mtOGG1 expression impacts age-associated neuroinflammatory pathways. Interestingly, the male mice, but not females, showed more significant effects of the enhanced mtOGG1 expression.

mtOGG1 expression reduces inflammatory proteins in both cortex and hippocampus

We measured the levels of mitochondrial OGG1 across age and genotypes. Our western blot results indicate that both aged male and female mtOGG1^{Tg} mice have equal amounts of OGG1 present in mitochondria. Also, consistent with a previous report [18], we found an age-dependent decline in mitochondrial OGG1 in WT aged mice compared with WT young mice (Supp. Figure 2A). Our transcriptome analysis indicated specific altered inflammation-related gene expression patterns of mtOGG1 overexpression only exhibited in aged male mice. To this end, we analyzed multiple inflammatory markers by western blot using mice brain lysates. As seen in Figure 2A, mtOGG1^{Tg} male mice showed significant decreases in different inflammatory markers, including TNFα, NLRP3 and IBA1. Cleaved interleukin-1 beta (IL1β) showed a decreasing, but not significant trend compared to that in control aged mice ($P = 0.08$). Cyclic GMP-AMP synthase (C-Gas) stimulates inflammatory interferon gene pathways through activation of STING upon sensing cytoplasmic DNA. Activated pSTING regulates downstream proinflammatory genes including TNFα, IL1β and IL6 [29]. Interestingly, mtOGG1^{Tg} males displayed a significant decrease in pSTING levels compared to control mice, whereas females did not show any difference among all investigated markers between controls and mtOGG1^{Tg} mice (Figure 2A).

Abnormal neuroinflammation is associated with aging and is characterized by the accumulation of activated microglial cells [30]. We therefore evaluated the microglial activation marker, IBA1 in mtOGG1^{Tg} and control mice brain sections. As shown in Figure

2B and 2C, brain sections of mtOGG1^{Tg} male mice showed decreased IBA1 staining compared to control mice in both cortex and hippocampus, respectively. NeuN staining indicates that there was no difference in the number of mature neurons in hippocampus and cortex between mtOGG1 and control mice (Figure 2B and 2C). Consistent with our previous results, female mice did not show any difference in IBA1 or NeuN staining between mtOGG1^{Tg} and control (Supp. Figure 1A and B). These results indicate that mtOGG1 overexpression reduces neuroinflammation possibly by reducing pSTING activation.

mtOGG1 removes accumulation of 8-oxoG in aged male brain tissues

Oxidative stress and mitochondrial dysfunction have been implicated in aging and aging-related neurodegenerative disorders [31]. 8-oxoG accumulates on DNA in an age-dependent manner [32]. To determine if the increased inflammation in aged mice correlated with 8-oxoG content in the brain, we measured 8-oxoG levels in hippocampus and cortex of male brain tissue. Brain sections were treated with RNAse and immunofluorescence staining was performed using 8-oxoG antibody. As shown in Figure 3A and 3B, aged mtOGG1^{Tg} male mice showed significantly decreased levels of 8-oxoG staining in both the hippocampus and cortex regions compared to control counterparts. We also investigated structural integrity and mitochondrial length in brain tissues of mtOGG1^{Tg} and control aged mice by electron microscopy. Figure 3C shows that mtOGG1^{Tg} male mice have normal mitochondrial length, aspect ratio and more cristae than control aged male mice. mtOGG1 expression did not improve mitochondrial structure in female mice (Supp. Figure 2). These data suggest that mitochondrial expression of 8-oxoG helps remove age associated accumulation of 8-oxoG and has a protective mitochondrial role in aged mouse models.

mtOGG1 expression in human microglial (HMC3) cells decreases the inflammatory response by reducing cytosolic accumulation of mtDNA

To investigate how mtOGG1 regulates the inflammatory response, we generated HMC3 cells stably expressing Myc-tagged OGG1 with a mitochondrial targeting sequence (COX8) (Figure 4A left panel). Inflammation was induced using LPS for 6 h and then cell lysates were prepared for western blot analysis. As shown in Figure 4A (right panel), treatment with LPS induced STING activation as evidenced by phosphorylation (pSTING) and other pro-inflammatory interleukins in the control cells. Notably, mtOGG1-expressing cells were resistant to LPS-induced STING activation and display reduced pro-inflammatory cytokines and TNFα compared to control cells after LPS treatment at both protein and mRNA levels (Figure 4B and 4C). As discussed above, cytosolic DNA can stimulate pro-inflammatory response through STING activation. Hence, we measured cytosolic DNA by immunofluorescence using dsDNA antibody. The mtOGG1 expressing cells had reduced LPS-induced dsDNA accumulation in the cytoplasm as compared to the mock control (Figure 4D). We further explored the possibility that mtOGG1 expression reduces release of mtDNA into cytoplasm, since liberated mtDNA can induce STING dependent inflammation [33]. Cells expressing mtOGG1 and vector were fractionated into mitochondrial and cytosolic fractions to quantify the level of mitochondrial specific DNA (MT-ND1, D-loop, MT-CO2, and MT-ATP6). Results shown in Figure 4E indicate that upon LPS treatment mtDNA is enriched more in cytoplasmic than in mitochondrial fraction. When compared to the mock cells response, mtOGG1 expression significantly reduced the release of mtDNA

into the cytosolic fraction. High-throughput analysis of 8-oxoG levels in mitochondrial DNA indicated that mtOGG1 expression significantly decreased LPS induced mtDNA 8-oxoG levels compared to control treated with LPS (Supp. Figure 4). These results indicate that enhanced expression of mtOGG1 decreases inflammatory responses by reducing the amount of 8-oxoG load in mtDNA and mtDNA in the cytoplasm.

Enhanced mtOGG1 expression improves mitochondrial health and upregulates metabolic pathways

To assess whether enhanced mtOGG1 expression improves mitochondrial functions, we measured the OCR in live cells using the Seahorse XF96 analyzer. The OCR was measured under basal conditions followed by the sequential addition of oligomycin (ATP synthase inhibitor), carbonyl cyanide 4-(trifluoromethoxy) phenylhydrazone (FCCP; mitochondrial uncoupler), and rotenone plus antimycin A (Complex I and III inhibitor) to assess ATP-linked and non-mitochondrial respiration, respectively. Consistently, treatment with LPS reduced both basal respiration and ATP-linked respirationin control cells. In contrast, LPS-treated mtOGG1 expressing cells showed improved basal respiration, ATP-linked and non-mitochondrial respiration compared to controls treated with LPS (Figure 5A–D). Further, mtOGG1 expression also decreased LPS-induced ROS generation in mitochondria (Figure 5E) and improved the mitochondrial membrane potential compared to similarly treated mock cells (Figure 5F). Importantly, we did not observe any change in mitochondrial content between mock and mtOGG1 expressing cells (Figure 5G). Mitochondria play a central role in energy metabolism and biosynthetic processes. Thus, we carried out transcriptomic analysis using the NanoString metabolism panel for metabolic pathways and found significantly upregulated terms including arginine metabolism and IDH12 activity in the hippocampus of mtOGG1^{Tg}mtOGG1^{Tg} male mice compared to WT (Figure 5H). Notably, mtOGG1^{Tg} mice showed lower pathway scores in cell cycle, cytokine/chemokine signaling, and TCR/costimulatory signaling terms compared with control mice (Figure 5H). Consistent with our previous data, the mtOGG1 expression did not show any significant effects in female mice model (Supp. Figure 3). These results suggest that mtOGG1 plays a protective role against age-associated decline in mitochondrial health and functions.

DISCUSSION

Higher steady state levels of 8-oxoG accumulation in different tissues during aging may be due to the inability of the DNA repair system to handle the increasing load. An age-dependent decline in the OGG1 expression and its import into mitochondria indicate that mitochondrial OGG1 plays an important role in mitochondrial dysfunction[17, 18]. mtDNA released from oxidatively-stressed mitochondria triggers inflammation via the c-GAS-STING pathway[27]. A recent study demonstrated that mice expressing mtOGG1 show resistance to the LPS-induced inflammatory response. They also showed that mtOGG1 expression limits the release of oxidized mtDNA into the cytoplasm, which activates inflammation [34]. mtOGG1^{Tg} mice show protection against diet-induced obesity, insulin resistance, and inflammation [25]. In this study, we show that mice expressing mitochondrial OGG1 are resistant to age-dependent neuroinflammation, and this effect is sex-dependent. Young male mice have been used in most of the studies conducted so

far. The greatest contribution of our study is that it shows how mtOGG1 is an effective protein against age-related cellular stress and neuro-inflammation using aged animals of both sexes. We showed that multiple inflammatory markers are significantly downregulated in male mtOGG1^{Tg} mice while females did not show a significant difference (Figure 2A). Interestingly, both male and female mtOGG1^{Tg} mice show decreased inflammation mediator genes like *Lcn2* (lipocalin 2), *Fos* (C-fos) and *Arc* (activity regulated cytoskeleton protein). However, female mtOGG1^{Tg} did not show any difference in inflammatory markers compared to WT aged mice. This indicates that these genes are affected by mtOGG1 expression irrespective of sexes but may not be involved in regulating inflammatory responses. We also explored the possibility that this sex-specific difference could be due to different mtOGG1 levels in aged mice. Interestingly, our western blot analysis indicates that there is no difference between the mitochondrial OGG1 levels in female and male mtOGG1^{Tg} aged mice (supp. Figure 2A). However, detailed pathway analysis indicates a clear difference in male and female responses to mtOGG1 expression. Male mtOGG1 Tg mice display decreased gene expression profile of key inflammatory pathways including adaptive immune response, innate immune response and inflammatory signaling (Figure 1C). They also exhibit better microglia function, astrocyte function, and growth factor signaling (Figure 1D). Female mtOGG1 Tg mice did not show any significant differences in these pathways. Further, Our results demonstrate that enhanced expression of mtOGG1 reduces the inflammatory response and 8-oxoG content in different regions of the brain in male but not in female mice, suggesting there is sex differences in the response of mtOGG1-regulated inflammation [35]. In humans, women generally live longer than men and have distinct genetic determinants of longevity. The best described explanations for these sex-specific differences are hormonal differences and sex chromosome-linked mechanisms[36]. Endocrine changes with aging can be caused by sex hormones. In addition to the dimorphic phenotype and gender characteristics, hormones also play vital roles in differential metabolic programming between males and females, which is manifested in many metabolic diseases during aging [37]. A previous study from our lab demonstrated that male mice exhibited impaired maximal brain mitochondrial respiration during oxidative phosphorylation, reduced glutathione peroxidase activity, and are more susceptible to mitochondrial oxidative damage than females following hypoxic ischemia [38]. This demonstrates sex-dependent mitochondrial respiratory function and oxidative damage responses may contribute to male susceptibility to mitochondrial dysfunction. On the other hand, this study approaches the problem from a different perspective and shows that mitochondrial repair mechanisms are more effective in male mice than in females.

Emerging evidence suggests that the c-GAS-STING pathway induces inflammation through sensing cytoplasmic DNA accumulation. In the cytoplasm, DNA fragments interact with c-GAS leading to STING phosphorylation at Ser365, which is required for the IRF3 mediated IFN response [39, 40]. This pathway is also activated in age-related neurodegeneration disorders such as Parkinson's and Alzheimer's diseases[41]. Here, we found that expression of mtOGG1 decreased STING activation and the inflammatory response (Figure 6). Our results also showed that overexpression of mtOGG1 reduced LPS-induced accumulation of mtDNA in the cytoplasm (Figure 6). This observation is in agreement with existing reports

demonstrating the aberrant release of mtDNA to cytoplasm due to cellular stress or injury triggers inflammatory responses in humans [42].

8-oxoG is one of the most abundant DNA modifications generated by reactive oxygen species. 8-oxoG is located in different gene regulatory regions, and OGG1 binding to 8-oxoG acts as a transcription regulator which induces allosteric G-quadruplex structure that recruits chromatin remodelers [43, 44]. Proinflammatory genes have high GC-content promoters, which are more vulnerable to being oxidized by oxidative stress [45]. OGG1 deficiency significantly reduces the induction of proinflammatory genes [46, 47]. Helleday et al. developed a selective active inhibitor for OGG1 (TH5487), which hampers OGG1 binding to 8-oxoG. Using this inhibitor, they show impaired OGG1 binding to guanine rich promoters of proinflammatory genes, including TNFα, which in turn decrease multiple pro-inflammatory genes [48]. Recently, they also developed a small molecule for OGG1 activation (TH10785). Cells treated with TH10785 show increased OGG1 recruitment at oxidative damage sites and increased repair [49]. In a separate study, Rumsey et al. demonstrated that 9-deaazagunaine activates OGG1 in an allosteric mechanism. Further, they also show that paraquat, as a highly effective and nonselective herbicide, mediated mitochondrial dysfunction can be normalized using OGG1 small molecule activators [50]. Thus, OGG1 small molecule activators may be used to improve mitochondrial function in oxidative stress-related diseases. It is now widely believed that regulation of inflammation could be a potential anti-aging intervention. Our results demonstrate that mtOGG1 is an important target in the aging-associated inflammation (Figure 6).

Thus, our study opens the door in understanding the role of base excision repair protein in brain aging and neurodegenerative diseases[51]. Increased 8-oxoG lesions were observed in the brains of neurodegenerative diseases, such as Alzheimer's Disease (AD) [52, 53], Parkinson's Disease(PD)[54], and Huntington's disease (HD)[55]. The level of OGG1 is also significantly decreased in AD brains[56, 57]. It is reported that mitochondrial OGG1 plays a vital role in neural stem cell viability and neuroprotection[19, 58, 59], which further influences cognition in the brains[60, 61]. Thus, restoration of mitochondrial deficits by increasing repair of oxidative DNA lesions using OGG1 small molecule activators has therapeutic application. Further studies will be necessary to address the role of mtOGG1 as possible players in aging and aging-associated disorders.

In summary, our study demonstrates that mitochondrial OGG1 plays important role in regulating age dependent neuroinflammation by maintaining mtDNA 8-oxoG levels and release of mtDNA to the cytoplasm, which subsequently activates the c-GAS/STING pathway.

Supplementary Material

Refer to Web version on PubMed Central for supplementary material.

ACKNOWLEDGEMENTS

mtOGG1^{Tg} mice were a gift from R. Stephen Lloyd, Oregon Health & Science University. We thank Drs. Tomasz Kulikowicz and Althaf Shaik for reading and providing helpful comments on the manuscript. We also thank Dr.

Beverly Baptiste for helping with the calculations. This work was supported by the Intramural Research Program of the National Institutes of Health, National Institute on Aging

REFERENCES

1. Ferrucci L, et al. , Proinflammatory state, hepcidin, and anemia in older persons. Blood, 2010. 115(18): p. 3810–6. [PubMed: 20081092]
2. Ferrucci L and Fabbri E, Inflammageing: chronic inflammation in ageing, cardiovascular disease, and frailty. Nat Rev Cardiol, 2018. 15(9): p. 505–522. [PubMed: 30065258]
3. Franceschi C, et al. , Inflamm-aging. An evolutionary perspective on immunosenescence. Ann N Y Acad Sci, 2000. 908: p. 244–54. [PubMed: 10911963]
4. Furman D, et al. , Chronic inflammation in the etiology of disease across the life span. Nat Med, 2019. 25(12): p. 1822–1832. [PubMed: 31806905]
5. Ridker PM, et al. , Antiinflammatory Therapy with Canakinumab for Atherosclerotic Disease. N Engl J Med, 2017. 377(12): p. 1119–1131. [PubMed: 28845751]
6. Walker KA, et al. , Connecting aging biology and inflammation in the omics era. J Clin Invest, 2022. 132(14).
7. Lodato MA, et al. , Aging and neurodegeneration are associated with increased mutations in single human neurons. Science, 2018. 359(6375): p. 555–559. [PubMed: 29217584]
8. Lu T, et al. , Gene regulation and DNA damage in the ageing human brain. Nature, 2004. 429(6994): p. 883–91. [PubMed: 15190254]
9. de Boer J, et al. , Premature aging in mice deficient in DNA repair and transcription. Science, 2002. 296(5571): p. 1276–9. [PubMed: 11950998]
10. Madabhushi R, Pan L, and Tsai LH, DNA damage and its links to neurodegeneration. Neuron, 2014. 83(2): p. 266–282. [PubMed: 25033177]
11. Kowald A and Kirkwood TB, Mitochondrial mutations, cellular instability and ageing: modelling the population dynamics of mitochondria. Mutat Res, 1993. 295(3): p. 93–103. [PubMed: 7689701]
12. Shenkar R, et al. , The mutation rate of the human mtDNA deletion mtDNA4977. Am J Hum Genet, 1996. 59(4): p. 772–80. [PubMed: 8808591]
13. Liguori I, et al. , Oxidative stress, aging, and diseases. Clin Interv Aging, 2018. 13: p. 757–772. [PubMed: 29731617]
14. Zhao MJ, et al. , Oxidative Stress Links Aging-Associated Cardiovascular Diseases and Prostatic Diseases. Oxid Med Cell Longev, 2021. 2021: p. 5896136. [PubMed: 34336107]
15. Nishioka K, et al. , Expression and differential intracellular localization of two major forms of human 8-oxoguanine DNA glycosylase encoded by alternatively spliced OGG1 mRNAs. Mol Biol Cell, 1999. 10(5): p. 1637–52. [PubMed: 10233168]
16. Minowa O, et al. , Mmh/Ogg1 gene inactivation results in accumulation of 8-hydroxyguanine in mice. Proc Natl Acad Sci U S A, 2000. 97(8): p. 4156–61. [PubMed: 10725358]
17. Tian F, et al. , Age-dependent down-regulation of mitochondrial 8-oxoguanine DNA glycosylase in SAM-P/8 mouse brain and its effect on brain aging. Rejuvenation Res, 2009. 12(3): p. 209–15. [PubMed: 19594329]
18. Szczesny B, et al. , Age-dependent deficiency in import of mitochondrial DNA glycosylases required for repair of oxidatively damaged bases. Proc Natl Acad Sci U S A, 2003. 100(19): p. 10670–5. [PubMed: 12960370]
19. Bo H, et al. , Exercise-induced neuroprotection of hippocampus in APP/PS1 transgenic mice via upregulation of mitochondrial 8-oxoguanine DNA glycosylase. Oxid Med Cell Longev, 2014. 2014: p. 834502. [PubMed: 25538817]
20. Zhao Y, et al. , DNA damage and repair in age-related inflammation. Nature Reviews Immunology, 2022: p. 1–15.
21. Moya GE, Rivera PD, and Dittenhafer-Reed KE, Evidence for the Role of Mitochondrial DNA Release in the Inflammatory Response in Neurological Disorders. Int J Mol Sci, 2021. 22(13).

22. Borsche M, et al. , Mitochondrial damage-associated inflammation highlights biomarkers in PRKN/PINK1 parkinsonism. Brain, 2020. 143(10): p. 3041–3051. [PubMed: 33029617]
23. Wang W, et al. , Mitochondrial DNA damage level determines neural stem cell differentiation fate. J Neurosci, 2011. 31(26): p. 9746–51. [PubMed: 21715639]
24. Klungland A, et al. , Accumulation of premutagenic DNA lesions in mice defective in removal of oxidative base damage. Proc Natl Acad Sci U S A, 1999. 96(23): p. 13300–5. [PubMed: 10557315]
25. Komakula SSB, et al. , The DNA Repair Protein OGG1 Protects Against Obesity by Altering Mitochondrial Energetics in White Adipose Tissue. Sci Rep, 2018. 8(1): p. 14886. [PubMed: 30291284]
26. Yuzefovych LV, et al. , Alteration of mitochondrial function and insulin sensitivity in primary mouse skeletal muscle cells isolated from transgenic and knockout mice: role of ogg1. Endocrinology, 2013. 154(8): p. 2640–9. [PubMed: 23748360]
27. Aarreberg LD, et al. , Interleukin-1beta Induces mtDNA Release to Activate Innate Immune Signaling via cGAS-STING. Mol Cell, 2019. 74(4): p. 801–815 e6. [PubMed: 30952515]
28. Hussain M, et al. , MITOL-dependent ubiquitylation negatively regulates the entry of PolgammaA into mitochondria. PLoS Biol, 2021. 19(3): p. e3001139. [PubMed: 33657094]
29. Paul BD, Snyder SH, and Bohr VA, Signaling by cGAS-STING in Neurodegeneration, Neuroinflammation, and Aging. Trends Neurosci, 2021. 44(2): p. 83–96. [PubMed: 33187730]
30. Candlish M and Hefendehl JK, Microglia Phenotypes Converge in Aging and Neurodegenerative Disease. Front Neurol, 2021. 12: p. 660720. [PubMed: 34025562]
31. Leon J, et al. , Corrigendum: 8-Oxoguanine accumulation in mitochondrial DNA causes mitochondrial dysfunction and impairs neuritogenesis in cultured adult mouse cortical neurons under oxidative conditions. Sci Rep, 2016. 6: p. 24696. [PubMed: 27128497]
32. Nie B, et al. , Age-dependent accumulation of 8-oxoguanine in the DNA and RNA in various rat tissues. Oxid Med Cell Longev, 2013. 2013: p. 303181. [PubMed: 23738036]
33. Sun B, et al. , Dengue virus activates cGAS through the release of mitochondrial DNA. Sci Rep, 2017. 7(1): p. 3594. [PubMed: 28620207]
34. Xian H, et al. , Oxidized DNA fragments exit mitochondria via mPTP- and VDAC-dependent channels to activate NLRP3 inflammasome and interferon signaling. Immunity, 2022. 55(8): p. 1370–1385 e8. [PubMed: 35835107]
35. Beery AK and Zucker I, Sex bias in neuroscience and biomedical research. Neurosci Biobehav Rev, 2011. 35(3): p. 565–72. [PubMed: 20620164]
36. Marais GAB, et al. , Sex gap in aging and longevity: can sex chromosomes play a role? Biol Sex Differ, 2018. 9(1): p. 33. [PubMed: 30016998]
37. Dearden L, Bouret SG, and Ozanne SE, Sex and gender differences in developmental programming of metabolism. Mol Metab, 2018. 15: p. 8–19. [PubMed: 29773464]
38. Demarest TG, et al. , Sex-dependent mitochondrial respiratory impairment and oxidative stress in a rat model of neonatal hypoxic-ischemic encephalopathy. J Neurochem, 2016. 137(5): p. 714–29. [PubMed: 27197831]
39. Chen Q, Sun L, and Chen ZJ, Regulation and function of the cGAS-STING pathway of cytosolic DNA sensing. Nat Immunol, 2016. 17(10): p. 1142–9. [PubMed: 27648547]
40. Liu S, et al. , Phosphorylation of innate immune adaptor proteins MAVS, STING, and TRIF induces IRF3 activation. Science, 2015. 347(6227): p. aaa2630. [PubMed: 25636800]
41. Hinkle JT, et al. , STING mediates neurodegeneration and neuroinflammation in nigrostriatal alpha-synucleinopathy. Proc Natl Acad Sci U S A, 2022. 119(15): p. e2118819119. [PubMed: 35394877]
42. Riley JS and Tait SW, Mitochondrial DNA in inflammation and immunity. EMBO Rep, 2020. 21(4): p. e49799. [PubMed: 32202065]
43. Xia L, et al. , CHD4 Has Oncogenic Functions in Initiating and Maintaining Epigenetic Suppression of Multiple Tumor Suppressor Genes. Cancer Cell, 2017. 31(5): p. 653–668 e7. [PubMed: 28486105]

44. Roychoudhury S, et al. , Endogenous oxidized DNA bases and APE1 regulate the formation of G-quadruplex structures in the genome. Proc Natl Acad Sci U S A, 2020. 117(21): p. 11409–11420. [PubMed: 32404420]
45. Wang R, et al. , The roles of base excision repair enzyme OGG1 in gene expression. Cell Mol Life Sci, 2018. 75(20): p. 3741–3750. [PubMed: 30043138]
46. Ba X, et al. , 8-oxoguanine DNA glycosylase-1 augments proinflammatory gene expression by facilitating the recruitment of site-specific transcription factors. J Immunol, 2014. 192(5): p. 2384–94. [PubMed: 24489103]
47. Pan L, et al. , Oxidized Guanine Base Lesions Function in 8-Oxoguanine DNA Glycosylase-1-mediated Epigenetic Regulation of Nuclear Factor kappaB-driven Gene Expression. J Biol Chem, 2016. 291(49): p. 25553–25566. [PubMed: 27756845]
48. Visnes T, et al. , Small-molecule inhibitor of OGG1 suppresses proinflammatory gene expression and inflammation. Science, 2018. 362(6416): p. 834–839. [PubMed: 30442810]
49. Michel M, et al. , Small-molecule activation of OGG1 increases oxidative DNA damage repair by gaining a new function. Science, 2022. 376(6600): p. 1471–1476. [PubMed: 35737787]
50. Tian G, et al. , Small molecule-mediated allosteric activation of the base excision repair enzyme 8-oxoguanine DNA glycosylase and its impact on mitochondrial function. Sci Rep, 2022. 12(1): p. 14685. [PubMed: 36038587]
51. Madabhushi R, Pan L, and Tsai L-H, DNA damage and its links to neurodegeneration. Neuron, 2014. 83(2): p. 266–282. [PubMed: 25033177]
52. Lovell MA and Markesbery WR, Ratio of 8-hydroxyguanine in intact DNA to free 8-hydroxyguanine is increased in Alzheimer disease ventricular cerebrospinal fluid. Archives of neurology, 2001. 58(3): p. 392–396. [PubMed: 11255442]
53. Pao P-C, et al. , HDAC1 modulates OGG1-initiated oxidative DNA damage repair in the aging brain and Alzheimer's disease. Nature communications, 2020. 11(1): p. 1–17.
54. Shimura-Miura H, et al. , Increased 8-oxo-dGTPase in the mitochondria of substantia nigral neurons in Parkinson's disease. Annals of neurology, 1999. 46(6): p. 920–924. [PubMed: 10589547]
55. Siddiqui A, et al. , Mitochondrial DNA damage is associated with reduced mitochondrial bioenergetics in Huntington's disease. Free Radical Biology and Medicine, 2012. 53(7): p. 1478–1488. [PubMed: 22709585]
56. Mao G, et al. , Identification and characterization of OGG1 mutations in patients with Alzheimer's disease. Nucleic acids research, 2007. 35(8): p. 2759–2766. [PubMed: 17426120]
57. Iida T, et al. , Expression of 8-oxoguanine DNA glycosylase is reduced and associated with neurofibrillary tangles in Alzheimer's disease brain. Acta neuropathologica, 2002. 103(1): p. 20–25. [PubMed: 11837743]
58. Wang W, et al. , Mitochondrial DNA damage level determines neural stem cell differentiation fate. Journal of Neuroscience, 2011. 31(26): p. 9746–9751. [PubMed: 21715639]
59. Cardozo-Pelaez F, Cox DP, and Bolin C, Lack of the DNA repair enzyme OGG1 sensitizes dopamine neurons to manganese toxicity during development. Gene Expression The Journal of Liver Research, 2005. 12(4–5): p. 315–323.
60. Hofer T, et al. , Restoration of cognitive performance in mice carrying a deficient allele of 8-oxoguanine DNA glycosylase by X-ray irradiation. Neurotoxicity Research, 2018. 33(4): p. 824–836. [PubMed: 29101721]
61. Shao C, et al. , Altered 8-oxoguanine glycosylase in mild cognitive impairment and late-stage Alzheimer's disease brain. Free Radical Biology and Medicine, 2008. 45(6): p. 813–819. [PubMed: 18598755]

Highlights:

- mtOGG1^{Tg} male mice show decreased age associated neuroinflammation compared to WT
- Cells expressing mtOGG1 display resistance to LPS induced STING activation and inflammatory response
- mtOGG1 expression reduce cytosolic mtDNA and mitochondrial 8-oxoG levels.

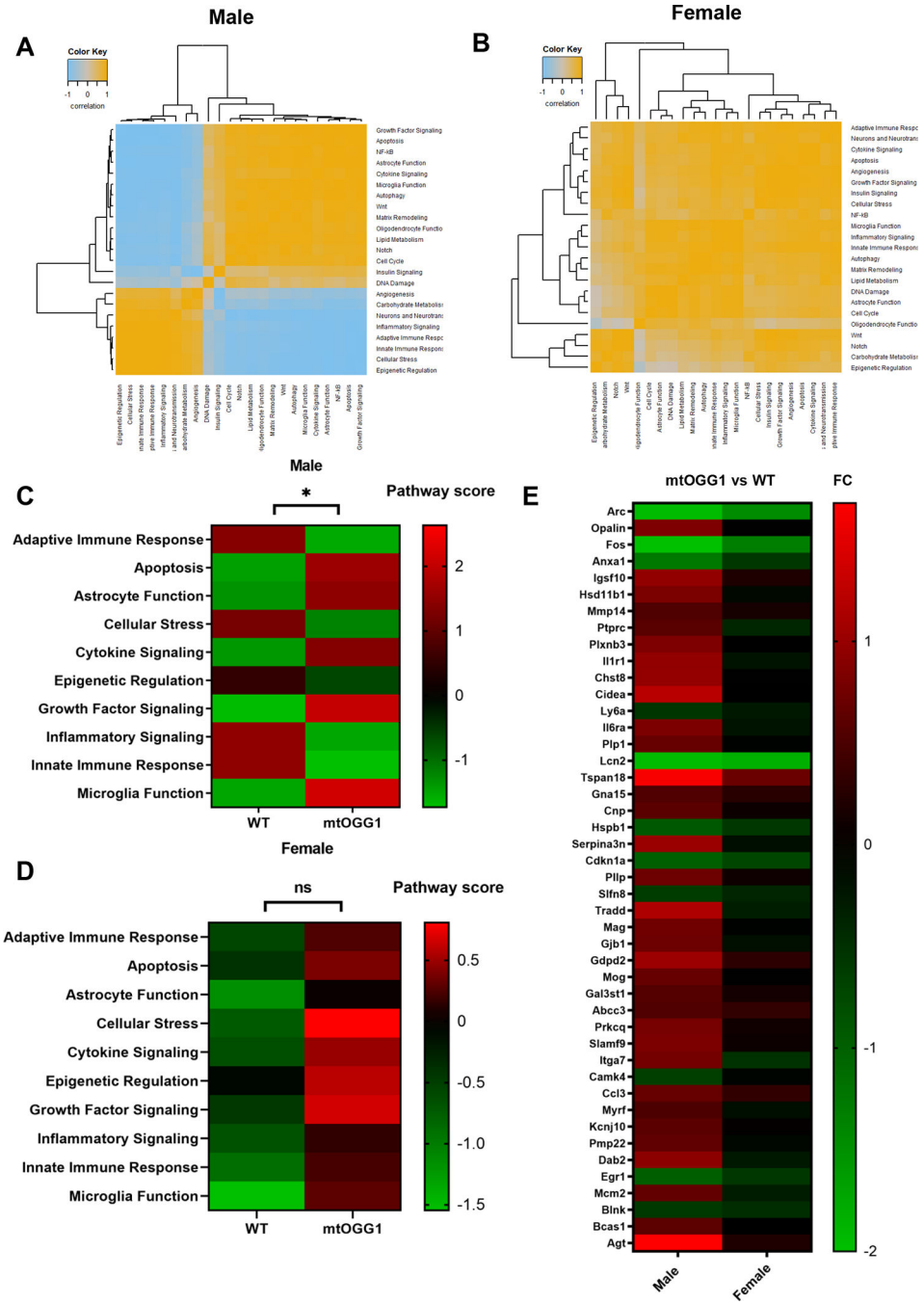

Figure 1: Enhanced mitochondrial expression of OGG1 exhibits reduced inflammation-related pathways in aged male hippocampus.

(A) and (B) Heatmap showing the correlation matrix of pathway scores defined by NanoString neuroinflammation panel. Orange and blue indicate positive and negative correlations, respectively. (C) and (D) Pathway scores were plotted against genes for different pathways including inflammatory signaling, growth factor signaling, astrocyte function, innate immune response, adaptive immune response, and cellular stress of male and female respectively. n=3 mice per group. All statistical significance was calculated by Student's t test. Data are shown as mean ± SD. *p < 0.05, **p < 0.01, ***p < 0.001. (E) The

set of significantly changed genes (p-value ≤0.05) in aged mtOGG1^{Tg} and control mice for both males and females.

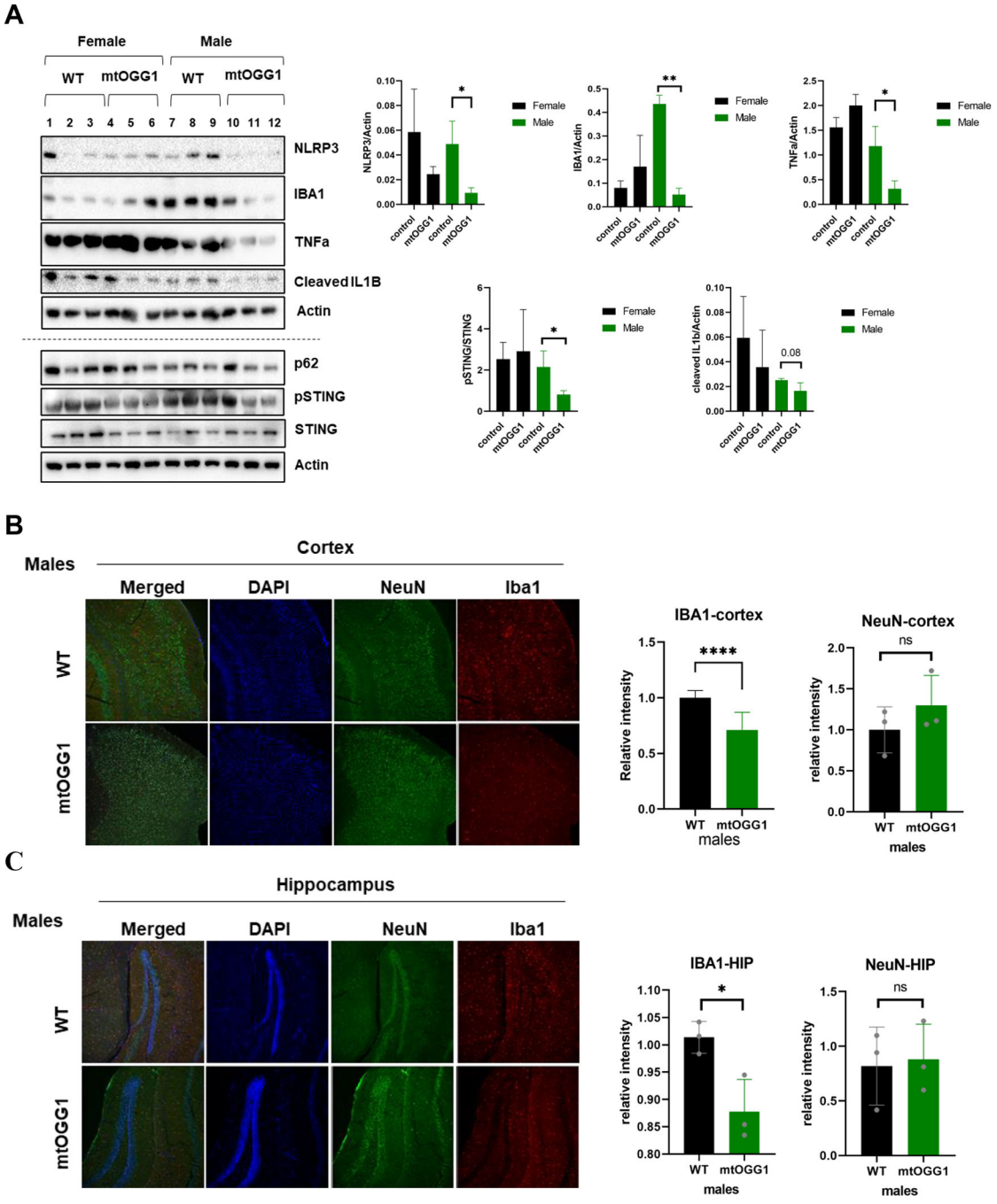

Figure 2: mtOGG1^{Tg} male mice show decreased inflammatory markers.

(A) Western blot analyses showing protein levels of NLRP3, IBA1, TNFα, cleaved IL1B, P62, pSTING, STING and actin as the loading control. The right panel shows the quantitation of protein levels. n=3 mice per group. (B) Representative immunostaining images of IBA1 (red), NeuN (green), and DAPI (blue) in mouse cortex. The right-side panel indicates the quantitation of IBA1 and NeuN intensity. n=3 mice per group. (C) Representative immunostaining images of IBA1 (red), NeuN (green) and DAPI (blue) in mouse hippocampus. The right-side panel indicates the quantitation of IBA1 and NeuN

intensity. n=3 mice per group. All statistical significance was calculated by Student's t test. Data are shown as mean ± SD. *p < 0.05, **p < 0.01, ***p < 0.001.

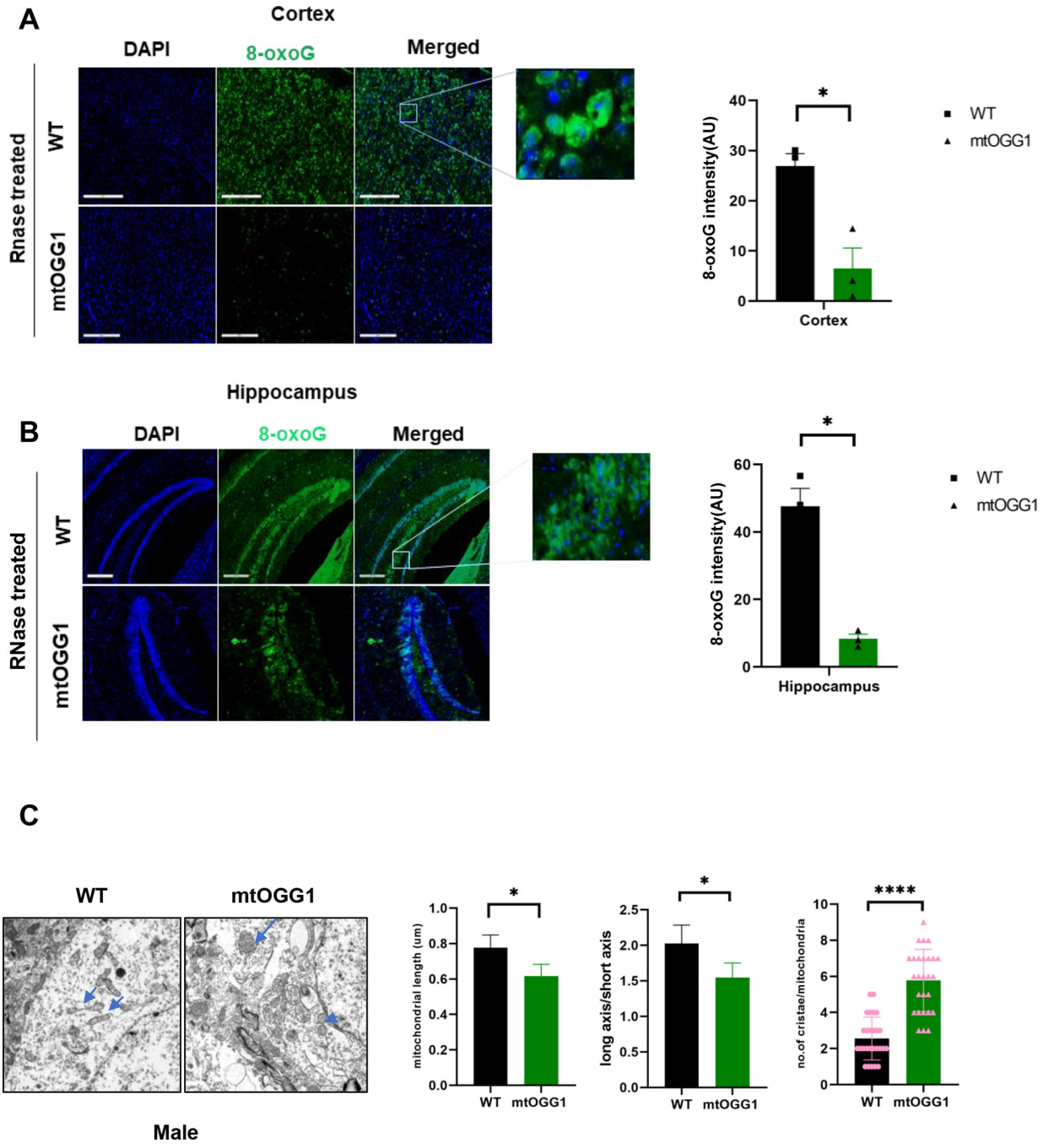

Figure 3: Enhanced mitochondrial expression of OGG1 removes accumulation of 8-oxoG in aged mouse brain.

(A) Representative immunostaining of 8-oxoG (green) and DAPI (blue) in mouse cortex. The right panel shows the quantitation of 8-oxoG intensity. n=3 mice per group. (B) Representative immunostaining of 8-oxoG (green) and DAPI (blue) in mouse hippocampus. The right panel shows the quantitation of 8-oxoG intensity. n=3 mice per group. (C) Representative mitochondrial images by electron microscopy from male brain tissues. The right panel shows the quantitation of mitochondrial parameters from electron microscopy.

n=3 mice per group. All statistical significance was calculated by Student's t test. Data are shown as mean ± SD. *p < 0.05, **p < 0.01, ***p < 0.001.

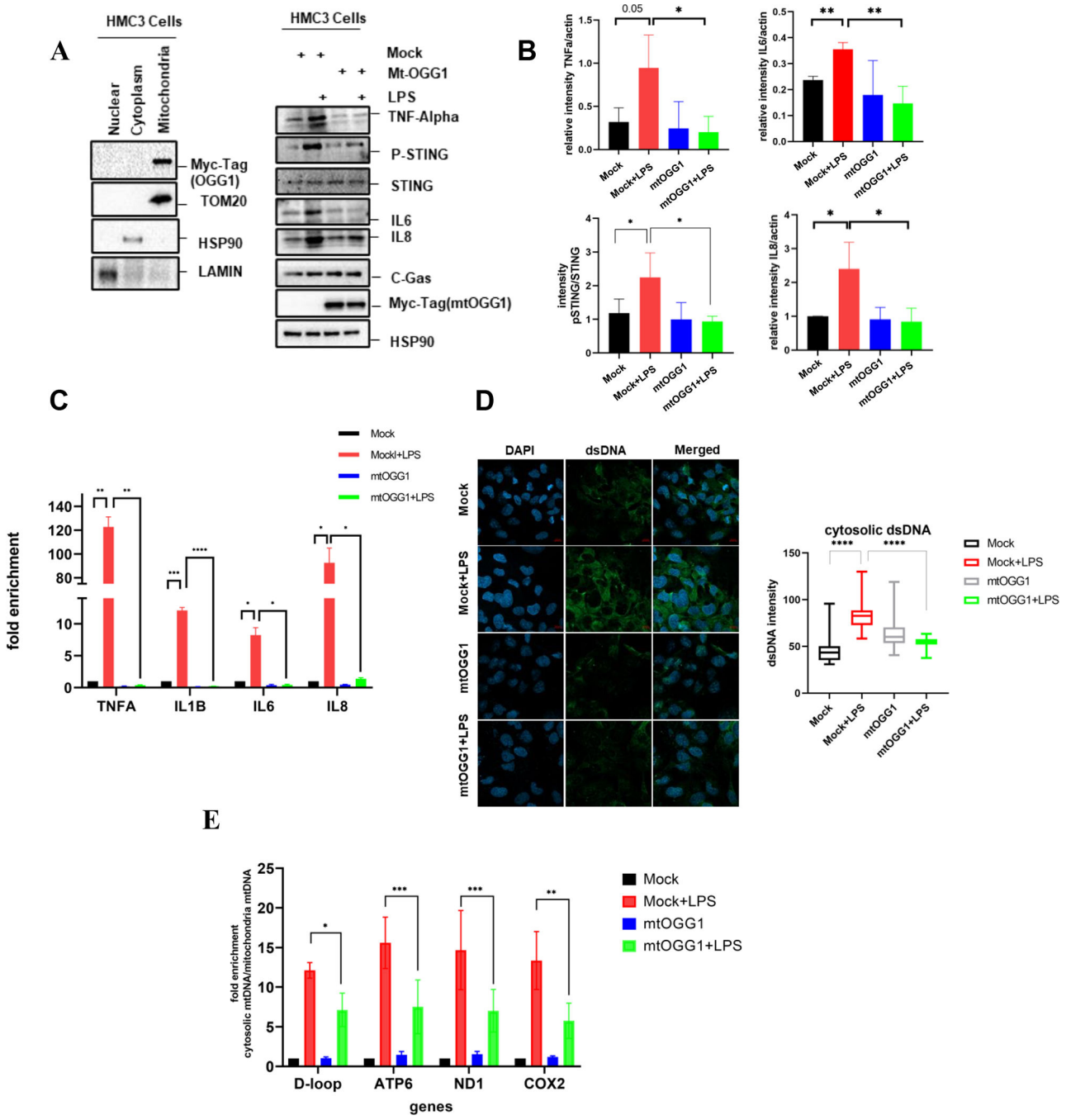

Figure 4: Enhanced mitochondrial expression of OGG1 regulates the release of mtDNA into cytoplasm.

(A) Purified mitochondrial, cytosolic, and nuclear fractions were prepared from HMC3 cells expressing Myc-Tag mtOGG1. In the left panel, TOM20, HSP90, and LAMIN were used as the mitochondrial, cytosolic, and nuclear markers, respectively. The right panel shows lysates prepared from HMC3 cells expressing empty vector (mock) or mtOGG1 with or without treatment of LPS. Western blot was carried out using antibodies against TNFα, pSTING, STING, IL6, IL8, C-Gas, Myc-Tag mtOGG1 and HSP90 as the loading control. (B) Quantitation of western blot (A). (C) qPCR analysis in HMC3 cells expressing vector

or mtOGG1 for the relative gene expression of pro-inflammatory genes, including TNFα, IL1B, IL6 and IL8 in the presence and absence of LPS. (D) Representative immunostaining of dsDNA(green) and DAPI (blue) in HMC3 cells expressing vector or mtOGG1 with or without LPS treatment. Total DNA was harvested from cytosolic and mitochondrial fractions of human fibroblasts and analyzed by qPCR. Cytosolic mtDNA genes were normalized to respective mitochondrial mtDNA genes (mt-ND1, D-loop, MTCO2, MT-ATP6) and presented as fold enrichment over vehicle-treated controls). Each experiment shows the average of results obtained in triplicate for each cell line. All statistical significance was calculated by Student's t test. Data are shown as mean ± SD. *$p < 0.05$, **$p < 0.01$, ***$p < 0.001$.

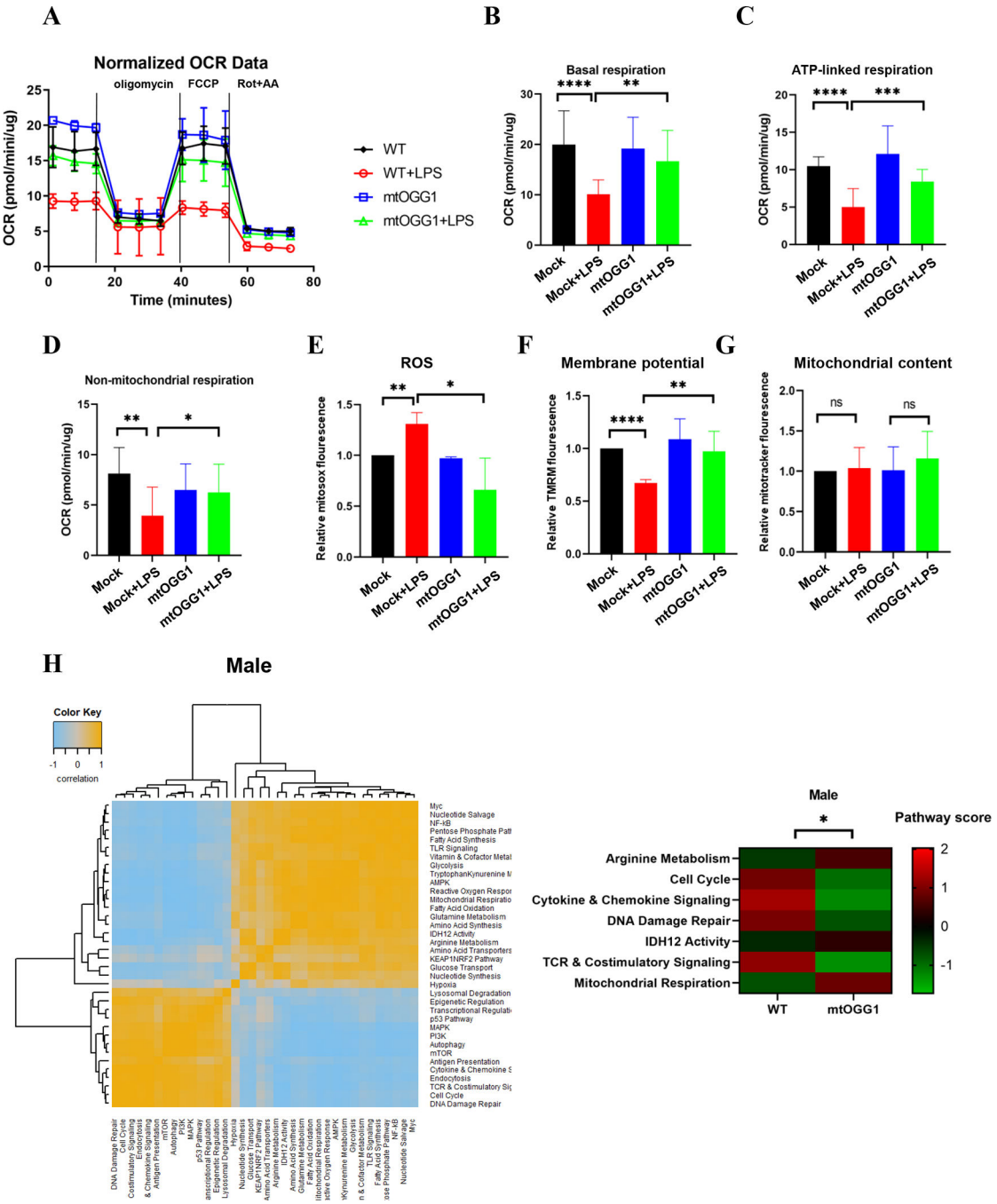

Figure 5: mtOGG1 improves mitochondrial metabolism.

(A-D) OCR in cells expressing mtOGG1 and controls treated with or without LPS (A), (B) OCR linked basal respiration, (C) ATP-linked respiration, (D) non-mitochondrial respiration data are normalized to protein levels, n=3. (E-G) Results of flow cytometry-based measurements of the indicated parameters: Mitochondrial ROS (E), membrane potential (F) and mitochondrial content (G). (H) Heatmap showing the correlation matrix of pathway scores defined by Nanostring metabolism panel between control vs mtOGG1 aged male mice. Orange and blue indicate positive and negative correlation, respectively (left panel).

Pathway scores are plotted against genes for different metabolic pathways like Arginine metabolism, cell cycle, cytokine and chemokine signaling, IDH12 activity and TCR and costimulatory signaling (right panel). Each experiment shows the average of results obtained in triplicate for each cell line. All statistical significance was calculated by Student's t test. Data are shown as mean ± SD. *$p < 0.05$, **$p < 0.01$, ***$p < 0.001$.

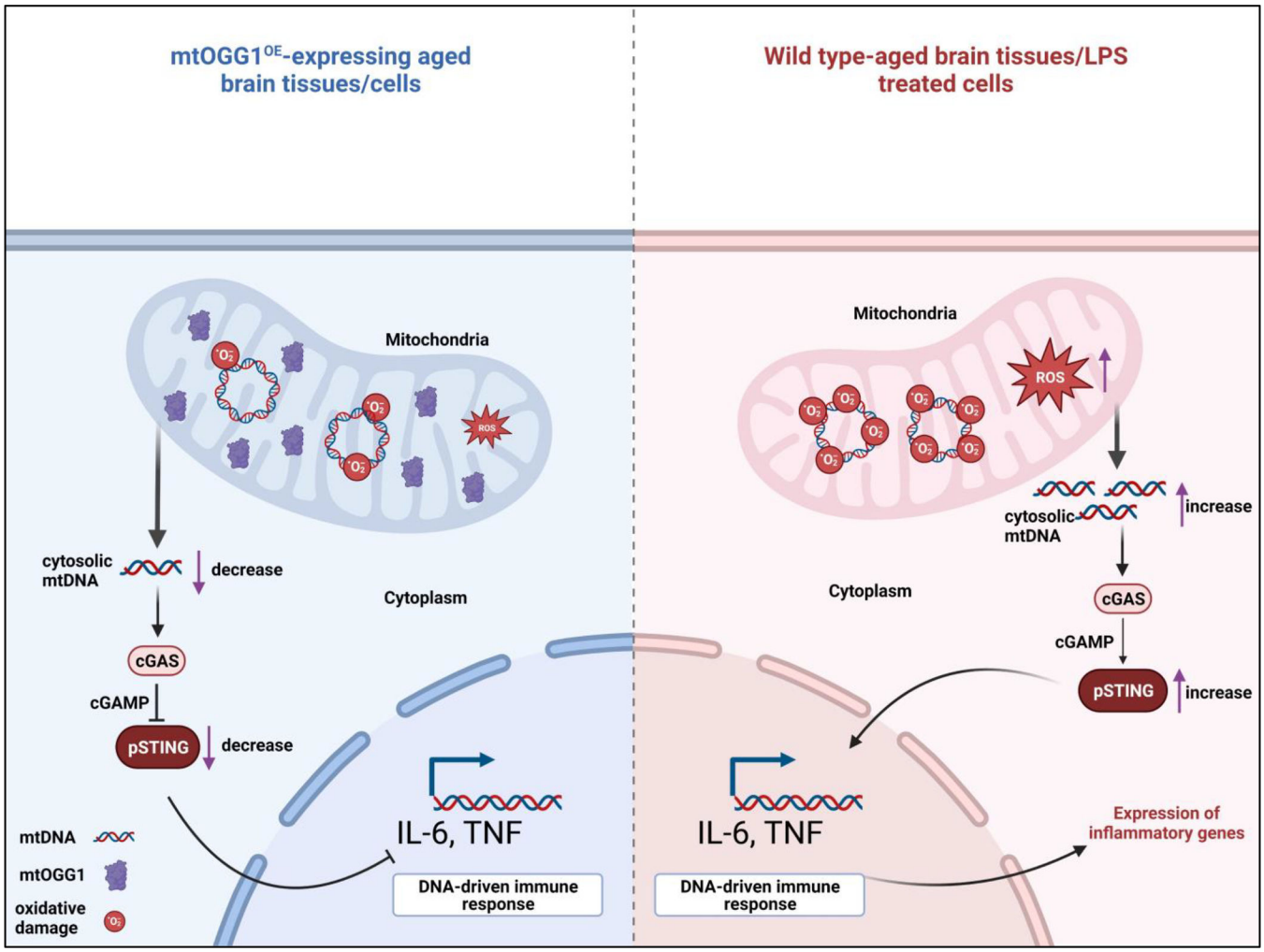

Figure 6: Graphical abstract. mtOGG1 expression reduces aging associated neuroinflammation.

Aged brain tissues of male mice or LPS treated human microglial cells display more cytosolic mtDNA followed by activation of STING and downstream inflammatory response. However, mtOGG1 expression decreased cytosolic mtDNA levels and prevent STING mediated inflammation.